INL/CON-16-37676
PREPRINT

Pellet Cladding Mechanical Interaction Modeling Using the Extended Finite Element Method

Top Fuel 2016

Benjamin W. Spencer, Wen Jiang,
John E. Dolbow, Christian Peco

September 2016

The INL is a
U.S. Department of Energy
National Laboratory
operated by
Battelle Energy Alliance

Pellet Cladding Mechanical Interaction Modeling Using the Extended Finite Element Method

Benjamin W. Spencer[1], Wen Jiang[1], John E. Dolbow[2], Christian Peco[2]

[1]*Fuel Modeling and Simulation Department, Idaho National Laboratory, Idaho Falls, ID 83415-0340*
[2]*Civil and Environmental Engineering Department, Duke University, Durham, NC 27708-0287*
+1-208-526-1683, benjamin.spencer@inl.gov

Abstract. Fracturing of ceramic light water reactor (LWR) fuel has multiple important effects on fuel performance. One particularly important concern is that cracks in the fuel cause elevated stresses in the cladding when pellet cladding mechanical interaction (PCMI) occurs. Modeling the effects of these cracks on the cladding stress is important for avoiding conditions when these elevated stresses could cause cladding failure. This can be readily done in fuel performance codes based on the finite element method by creating finite element meshes that incorporate discrete cracks defined *a priori*. The drawback of this approach, however, is that the crack geometry must be pre-determined rather than computed by the computational model.

The extended finite element method (XFEM) is a powerful method to represent arbitrary propagating discrete cracks in finite element models. The use of XFEM has been previously demonstrated for modeling propagating discrete cracks in the BISON fuel performance code. This paper demonstrates an initial application of XFEM to model stress concentrations induced by fuel fractures at the fuel/cladding interface during PCMI. This is demonstrated on a study of a pre-defined stationary crack in a 2D cross-section model of a LWR fuel rod. The results from a model with a discrete crack defined with XFEM compare favorably with the results from a model with the same crack geometry defined in the finite element mesh. This study focuses on benchmarking the use of XFEM for PCMI modeling with a stationary crack, but this technique will be readily extended in the future to consider PCMI in conjunction with arbitrary, physics-driven crack propagation.

Keywords: PCMI, XFEM, fracture, simulation

INTRODUCTION

As a brittle material, the ceramic UO_2 used as light water reactor fuel experiences significant fracturing throughout its life, beginning with the first rise to power of fresh fuel. This has multiple effects on the thermal and mechanical response of the fuel/cladding system. One such effect that is particularly important is that when there is mechanical contact between the fuel and cladding, cracks that extending from the outer surface of the fuel into the volume of the fuel cause elevated stresses in the adjacent cladding, which can potentially lead to cladding failure.

Modeling the thermal and mechanical response of the cladding in the vicinity of these surface-breaking cracks in the fuel can provide important insights into this behavior to help avoid operating conditions that could lead to cladding failure. Such modeling has traditionally been done in the context of finite-element-based fuel performance analysis by modifying the fuel mesh to introduce discrete cracks [1]. While this approach is effective in capturing the important behavior at the fuel/cladding interface, there are multiple drawbacks to explicitly incorporating the cracks in the finite element mesh. Because the cracks are incorporated in the original mesh, the mesh must be modified for cracks of specified location and depth, so it is difficult to account for crack propagation and the formation of new cracks at other locations.

The extended finite element method (XFEM) has emerged in recent years as a powerful method to represent arbitrary, evolving, discrete discontinuities within the context of the finite element method [2,3]. XFEM can be used to represent a variety of discontinuity types, including jumps in the solution fields caused by fractures, material interfaces, or solution domain boundaries. Development work is underway by the authors to implement XFEM in the BISON fuel performance code, and this capability has previously been demonstrated in simulations of fracture propagation in ceramic nuclear fuel [4]. These prior simulations included only the fuel, and excluded the cladding for simplicity. Figure 1 shows representative results from a fracture propagation analysis on a 2D cross section model of fresh LWR fuel subjected to an initial ramp to full power where cracks are modeled with XFEM in the BISON code. These results highlight the ability of this technique to model fractures that can propagate during the analysis, and which can pass arbitrarily through the finite element mesh, independent of element boundaries.

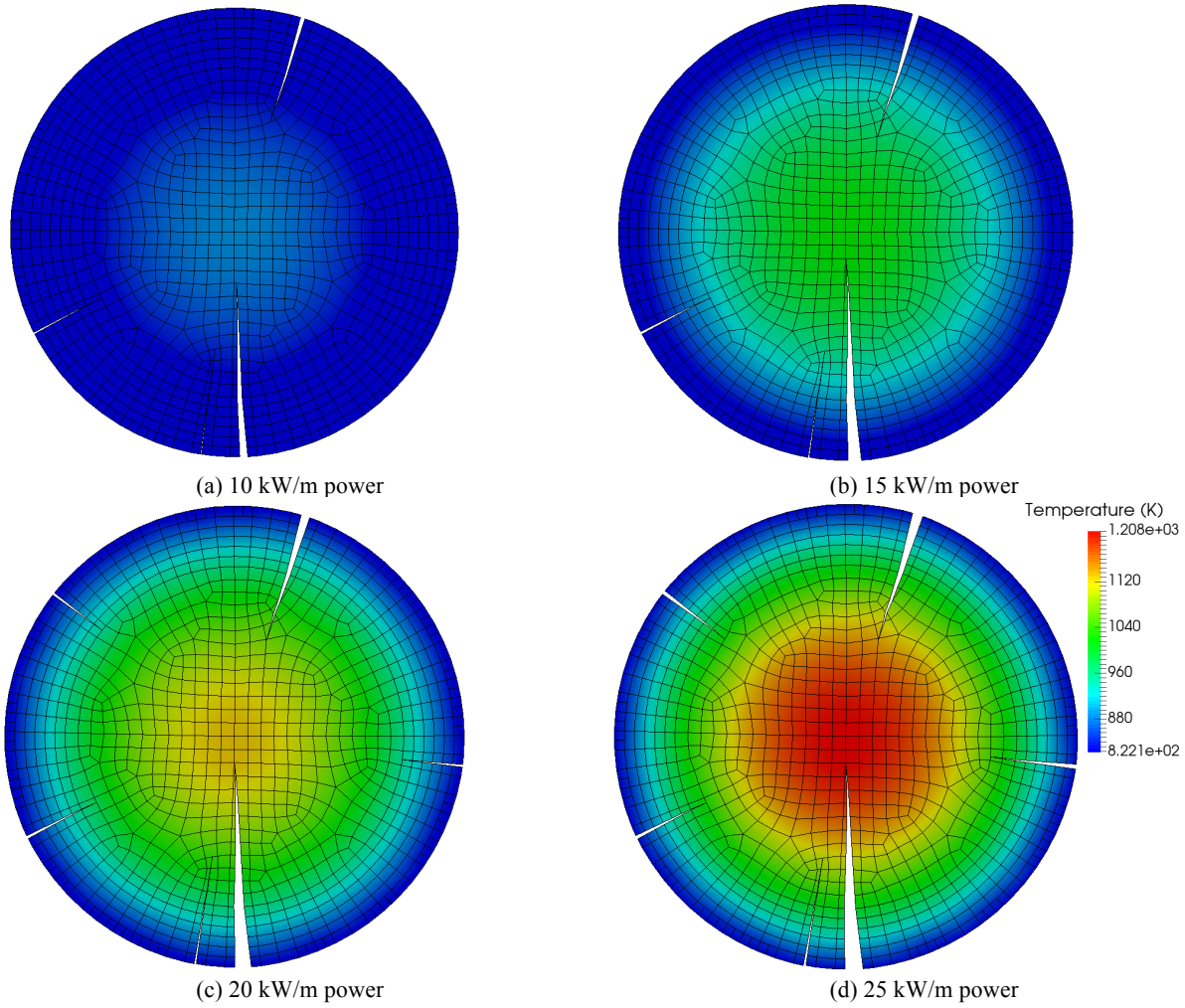

(a) 10 kW/m power (b) 15 kW/m power

(c) 20 kW/m power (d) 25 kW/m power

FIGURE 1. Representative results of a fracture propagation simulation in fresh LWR fuel ramped up to full (25 kW/m) power using XFEM to represent propagating discrete cracks in BISON derived from models presented in [4]. Temperature fields are shown on the mesh with magnified 10x for four different power levels during the power ramp.

There are multiple potential benefits to using the XFEM to represent discrete cracks in the fuel for studies on their effects on the cladding thermo-mechanical response during PCMI. One benefit is convenience in setting up models. To investigate multiple prescribed crack scenarios, there is no need to generate separate meshes. A single mesh with no cracks can be used for all scenarios, and discrete crack geometries are defined by the geometry of the cutting lines, which doesn't involve meshing. This is particularly beneficial for a 3D model, where generating meshes conforming to crack geometries can be challenging. Rather than studying the effects of prescribed stationary cracks

on PCMI, it would be preferable to study the effects of cracks that have propagated based on physical considerations, which is permitted by the XFEM.

XFEM FOR FUEL PERFORMANCE SIMULATION

This paper demonstrates an initial application of the XFEM to model stress concentrations induced by fuel fractures at the fuel/cladding interface during PCMI. The formulation and implementation of this method are summarized below.

XFEM and Phantom Node Methods

In the finite element method, the solution vector $\boldsymbol{u}$ at a given position, $\boldsymbol{x}$, and time, t, is interpolated from the nodal solution $\boldsymbol{u}_I$ using continuous shape functions N_I:

$$\boldsymbol{u}(\boldsymbol{x},t) = \sum_{I=1}^{n} N_I(\boldsymbol{x})\boldsymbol{u}_I(t) \tag{1}$$

This works well for simulating physical phenomena that are spatially continuous, but breaks down when discontinuities arise in the solution field, as occurs during fracture. In a mechanics simulation, stresses are computed from strains, which are derivatives of the solution field. This is problematic when fractures occur because the jump in the displacement field is well defined, but the derivative is not.

XFEM introduces a discontinuity by enhancing the continuous solution field with a term using the Heaviside function H, which evaluates to 1 on one side of the discontinuity and 0 on the other [2,3]. Additional degrees of freedom corresponding to this enrichment $\boldsymbol{e}_I$ are added to all nodes whose basis is intersected by the discontinuity. With this enrichment, the otherwise continuous solution field of Equation 1 is expressed as:

$$\boldsymbol{u}(\boldsymbol{x},t) = \sum_{I=1}^{n} N_I(\boldsymbol{x})(\boldsymbol{u}_I(t) + H(\boldsymbol{x})\boldsymbol{e}_I(t)) \tag{2}$$

These enrichments are applied at arbitrary locations in the mesh independent of element boundaries; so discrete cracks can be introduced at locations that traverse finite elements. For fracture mechanics simulations, in addition to the Heaviside enrichment shown in Equation 2, higher-order enrichment terms are commonly included to represent the asymptotic fields near the crack tip. These terms are not used in the present work, although they could be included. Because the phenomena of interest in the present work occur far from the crack tip, there is no need to include those near-tip enrichment terms.

To implement the form of the XFEM defined by Equation 2 in a finite element code requires the ability to add additional degrees of freedom to the nodes of elements intersected by discontinuities. An alternative method to introduce discontinuities in solution fields known as the phantom node method [5] was proposed several years after the introduction of the XFEM. In the phantom node method, elements intersected by a crack are deleted and replaced by two elements that occupy the same physical locations as the original elements. A portion of the domain of each of these new elements (partial elements) represents physical material, while the remainder does not. The combined physical portions of the partial elements cover the entire domain of the original element that was split. The nodes that are connected to the non-physical portions of those elements are known as phantom nodes. The solution field is interpolated on the partial elements using the standard shape functions. When fields are integrated over partial elements, such as to compute an element's contribution to the residual, only the portion on the physical part of the element is considered. The main challenge in the phantom node method is developing an algorithm to correctly connect the partial elements split by a crack. Neighboring elements that share a common cracked edge should share physical and phantom nodes.

Shortly after the phantom node method was proposed, it was recognized [6] that it enriches the solution field in exactly the same way as does the originally proposed XFEM method when only the Heaviside enrichment term is included. Introducing cracks with the phantom node method results in the introduction of exactly the same number of new degrees of freedom to the equation system as does the original XFEM method, but those degrees of freedom correspond to standard solution field degrees of freedom rather than being special enrichment degrees of freedom. The phantom node method has been widely adopted as a technique to introduce Heaviside discontinuities of the

XFEM method because it is often more natural to implement in an existing code, and simplifies the process of applying multiple recursive cuts to an element, as occurs during crack branching or coalescing.

BISON XFEM Implementation

Because of the advantages of the phantom node method, it was used to develop an implementation of the XFEM in a fuel performance code. BISON is a finite element based fuel performance code under development at Idaho National Laboratory (INL) to simulate the performance of a variety of nuclear fuel forms, including LWR fuel [7]. BISON is often used to solve coupled thermal-mechanical models, but it is based on a general multiphysics solution framework that permits the inclusion of other coupled physics that effect fuel performance, such as species diffusion. The open-source MOOSE multiphysics framework [8], also developed at INL, forms the basis for BISON's flexible solution environment.

While the motivation for this work was to add capabilities to BISON, the phantom node method has been implemented in MOOSE, and is available for use for any code based on MOOSE, including BISON. In addition to the benefits of the phantom node method described previously, in a multiphysics solution environment, another benefit of the phantom node method is that when elements are split, all of the solution fields in a multiphysics simulation are automacially enriched. For a thermo-mechanical simulation, this means that both thermal and mechanical solution fields experience jumps across fractures. The following three primary developments, summarized below, were necessary to implement this capability:

Mesh Cutting Algorithm

The bulk of the computer code for a phantom node-based XFEM capability lies in the algorithm to create and connect the partial elements that are generated by cut planes passing through elements. Algorithms for fragmentation visualizations have been developed by the computer graphics community, and are applicable for this purpose. An algorithm based partly on the work of [9] was developed for the MOOSE XFEM implementation, and is briefly described here.

In this mesh cutting algorithm, the first phase is identifying element edges that are cut by fracture planes. These fracture planes can either be directly user-defined, as is the case in the present work, or defined by physics-based criteria such as stresses or fracture integrals to model propagating cracks.

Once the cut edges are identified, the elements to be split (those traversed by a fracture plane) are identified, and sets of fragments within those split elements are defined. These fragments define the boundaries of the physical portions of the partial elements that will be created. A new element is then created corresponding to each of these fragments, and one of these fragments is used to define the physical portion of each of the new elements.

The last phase of this algorithm is to join the common edges of neighboring fragment elements. A search is made through the neighbors of a given partial element to see if any of the neighbors should share a common edge. If they should share a common edge, the nodes on those neighboring elements are combined, so that continuity of the solution across that edge is ensured. Determinations of whether edges should be combined are based on whether the physical material for the two elements in consideration is contiguous across that common edge.

For each time step in the analysis, the mesh cutting algorithm is run to see whether cracks should propagate. If they do, the cutting algorithm deletes elements and replaces them with new partial elements. In the work presented here, only an initial mesh modification is done to cut the mesh to represent user-defined stationary cracks before the first time step in the analysis.

Partial Element Integration Algorithm

The other major modification made to the finite element code is that quadrature rules that are used to perform volume integrals, such as for computing the integral of the divergence of the stress tensor to compute an element's contribution to the residual, are adjusted to integrate over the physical portions of the cut elements. This is commonly done by forming a set of triangular (2D) or tetrahedral (3D) sub-elements that cover the entire physical portion of the split element's domain. These sub-elements are used only for integration, and new integration points are introduced at the locations of those sub-element's integration points.

A significant drawback of this sub-division approach to partial element integration is that when there is stateful material data at integration points (as is often the case for nonlinear mechanical constitutive models and a variety of other behavior models used in fuel performance analysis), this data must be mapped to the new integration points. To avoid this mapping of material data to new integration points, the approach taken in this work is to retain the original quadrature points, but scale their weights by a factor equal to the physical volume fraction of a split element. This does introduce some error, but this error decreases with mesh refinement, and has been shown in studies performed by the authors to be negligible for many practical applications.

Visualization of Partial Elements

Because the phantom node method represents cut elements with two overlapping partial elements, proper visualization of results with cut elements requires additional processing. If nothing is done, results on the displaced mesh will show overlapping elements in cut regions. Cracks would only be evident as gaps in the mesh with very large crack openings, and even then, the visualized cracks would not accurately represent the crack path (as shown in Figure 2(a)). Non-physical components of cut elements must be clipped off to properly visualize the results. A plugin to the ParaView[10] visualization software has been developed for this purpose. Figure 2(b) shows the results of applying this plugin to the cut mesh of Figure 2(a).

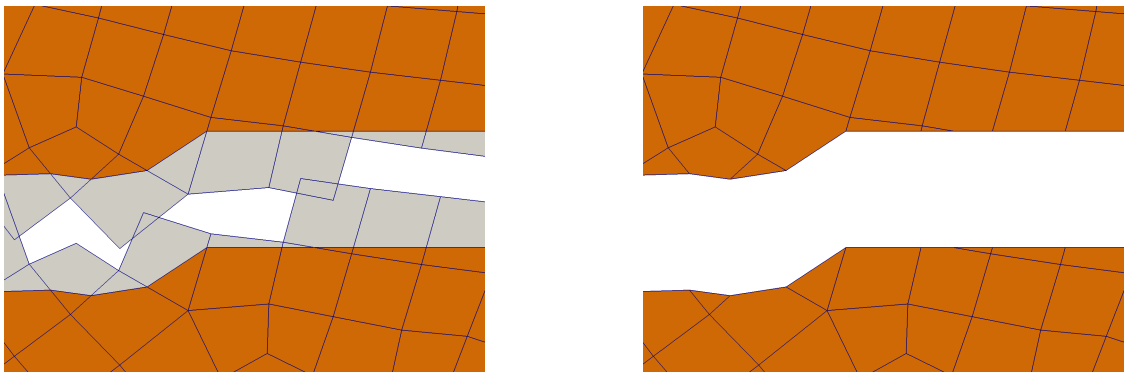

(a) Portion of cut mesh showing physical (dark) and non-physical (light) components of cut elements.

(b) Visualization of cut mesh with algorithm applied to hide non-physical portions of cut elements.

FIGURE 2. Demonstration of visualization filter applied to partial elements in the phantom node algorithm

Contact with XFEM

To model PCMI with the XFEM, contact interactions between cracked fuel and cladding, where the cracked fuel is represented by partial elements, must be represented. The contact algorithm must thus be able to handle interactions between a face of a partial element that is split by a cutting plane and an un-fractured element on the opposing contact surface.

BISON employs a master/slave, node on face algorithm to enforce mechanical contact constraints. This algorithm adds constraints that enforce that the nodes on the slave side of the contact interface do not penetrate the faces on the master side of the interface. The fuel is typically designated as the slave side of those interfaces. For thermal contact, BISON can use either a two-way algorithm that computes fluxes at integration points, or use a master/slave algorithm similar to that used for mechanical contact.

Within the phantom node method, the faces of the partial elements cut by fracture planes on the outer surface of the fuel contain a combination of physical and phantom nodes. The approach taken here to enforce contact on the partial elements is to simply add the phantom nodes to the set of nodes on which contact is enforced. The search algorithm locates the points on the opposing face for those points just as it does for physical nodes, and the same non-penetration constraints are applied. All of the nodes on the partial elements, especially the phantom nodes, have reduced thermal and mechanical stiffness associated with them because of the reduction in the physical volume of those elements. This results in a reduction of the mechanical contact force and integrated flux in the solution consistent with a reduction in the physical portion of the element.

This approach introduces small local errors because the point loads and integrated fluxes are applied to the master surface at the location of the phantom node rather than the point at the intersection of the cut plane and the slave surface. These errors have a minor effect on the results because they do not affect the overall force or flux across the contact surface, and their effects diminish with mesh refinement. Changing the location of the contact point to be at the edge of the physical material would certainly be preferable, and is a topic of future development.

SEPARATE EFFECTS BENCHMARKS OF THE XFEM WITH CONTACT

To gain confidence in the performance of the mechanical and thermal contact enforcement algorithms employed here, a set of small contact benchmark problems was developed. These problems all involve contact between two blocks, one of which is split by an XFEM interface. Displacement boundary conditions are imposed to pull the split block apart, and then put it in contact with the intact block.

The thermal variant of this test includes a displacement field in its solution only for the purpose of imposing mechanical displacement boundary conditions to pull the split block apart. The problem is intentionally set up with zero thermal expansion to ensure that there are no mechanical strains. Dirichlet boundary conditions are employed to prescribe temperatures on the far, non-contacting surfaces of the model. A temperature of 0.0 is imposed on the far left boundary, and a temperature of 1.0 is imposed on the far right boundary. Because these models are used for illustrative purposes, an arbitrary unit system is employed. Thermal contact constraints are imposed across the interface. When a horizontal split in the center of the left block is introduced using the XFEM, the material on the intact (right) side of the contact interface has an elevated temperature. This model was run in two ways: with the XFEM defining the split block, and with two separately meshed blocks on the split (left) side for a benchmark comparison. Figure 3 shows temperature contours for both cases, as well as a plot of the temperature along the surface of the intact block in contact with the split block. For the coarse mesh shown here, there are noticeable discrepancies between the XFEM and meshed crack results, but with one level of refinement in the vertical direction (splitting each element in the vertical direction into two elements), these differences become negligible.

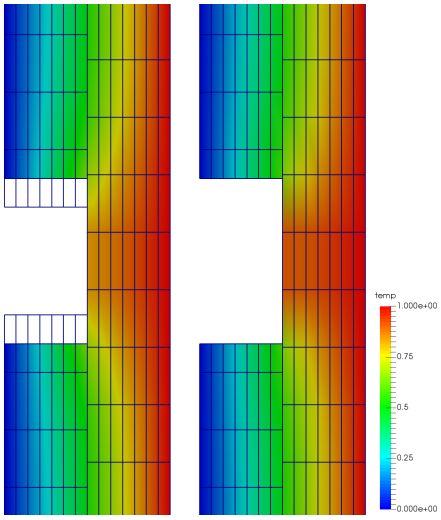

(a) Temperature contours on the XFEM model (left) and meshed crack model (right). Non-physical portions of split elements in the XFEM model are shown in white for illustrative purposes.

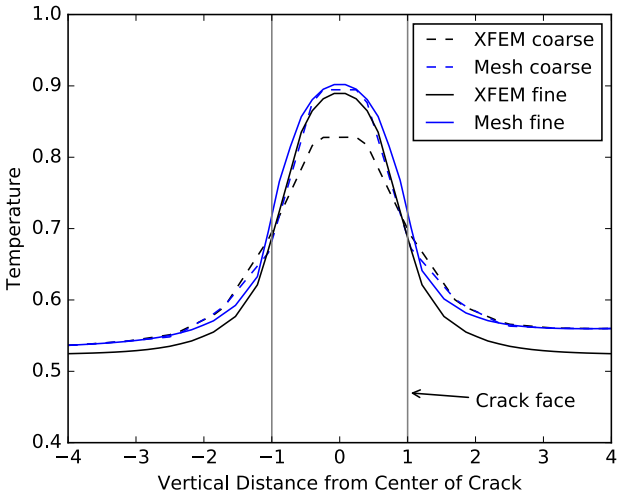

(b) Plot of temperature along a vertical line along the left surface of the block on the right (the intact block). The coarse mesh is the mesh shown in Figure 3(a). The fine mesh has twice the refinement level in the vertical direction.

FIGURE 3. Test of thermal contact comparing XFEM-derived results with results from a model with a meshed crack

A variant of this test was also developed for mechanical contact. The same two blocks are used, but in this case, Dirichlet boundary conditions are imposed in the horizontal direction on the far sides of the two blocks to cause mechanical interference between the blocks. The two blocks have unit widths, and an initial gap of 0.001 length units. The left side of the left block is held fixed, while the right side of the right block is moved to the left by 0.101 length units (enough to completely close the gap and have an interference equal to 1/10 the thickness of the two blocks. Contour plots of the displacement in the x-direction for the XFEM and meshed crack cases are shown in

Figure 4(a), and line plots of that displacement along the surface of the uncut block in contact with the split block are shown in Figure 4(b). As for the thermal case, there are noticeable discrepancies between the XFEM and meshed crack cases with the coarse mesh, but these decrease dramatically with one level of mesh refinement (although the differences with the refined mesh are still larger than those for the thermal case).

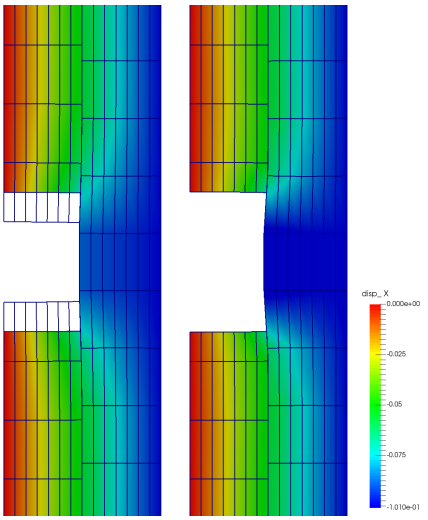

(a) X-direction displacement contours on the XFEM model (left) and meshed crack model (right). Non-physical portions of split elements in the XFEM model are shown in white for illustrative purposes.

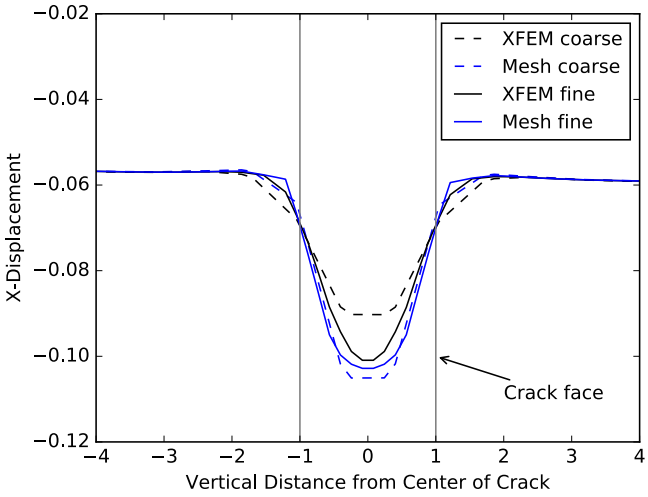

(b) Plot of x-direction displacement along a vertical line along the left surface of the block on the right (the intact block). The coarse mesh is the mesh shown in Figure 4(a). The fine mesh has twice the refinement level in the vertical direction.

FIGURE 4. Test of mechanical contact comparing XFEM-derived results with results from a model with a meshed crack

PCMI SIMULATION WITH THE XFEM

Once confidence has been gained in the ability of the contact algorithm to correctly represent thermal and mechanical contact between a volume cut by the XFEM and another volume, this approach can be applied to a nuclear fuel simulation. For this application, a 2D cross-section of a boiling water reactor (BWR) fuel pellet and cladding is subjected to representative BWR conditions. A quarter symmetry model with appropriate symmetry boundary conditions is employed. This model contains a single prescribed radial crack starting from the outer radius and terminating at a point with a radius from the centerline equal to half the outer radius. This model thus represents a fuel pellet containing four equally spaced radial cracks. Two versions of the model are studied here: one in which the crack has been included in the mesh, and one in which a stationary crack with the same geometry is represented with the XFEM.

This model is based on another model of a BWR fuel rod containing a defective pellet [10], and uses the same set of physical and behavior models, as well as loading conditions, as the model used in that study. It employs temperature and burnup-dependent models for thermal conductivity. A linear elastic model is used for the fuel constitutive behavior, in conjunction with a relocation model. The fuel incorporates models for volumetric swelling and contraction due to thermal expansion, gaseous swelling, solid swelling, and densification. A model that includes thermal and irradiation creep, as well as instantaneous plasticity, is employed for the cladding. Generalized plane strain conditions are imposed independently on the fuel and cladding to permit stress-free expansion of the fuel and cladding in the axial direction of the rod, but enforce that planar sections of the fuel and cladding remain planar. For the current study, the mechanical contact interaction between the fuel and pellet is considered to be frictionless. For realistic PCMI analysis, it is important to consider frictional effects. This will require additional development, and is a topic of ongoing work.

The evolution of the properties of the plenum gas over time is computed using a separate full-length 2D axisymmetric model of the full fuel rod. The full-length rod model computes the time history of the plenum gas mixture as a function of the fission gas released over the entire rod, as well as the time history of the plenum gas

pressure and temperature. These are input as boundary conditions into the 2D cross section model employed here. The power history imposed on this model is representative of conditions that would be experienced by a BWR rod that is irradiated for a first cycle in a position away from a control blade, and then moved to a position near a control blade. This location in the rod initially experiences suppressed power during the second power cycle, but is then subjected to a sudden increase to full power (25 kW/m) due to a control blade withdrawal, and is then also subjected to a ramp to high power (about 35 kW/M).

The results of the solution at the end of the analysis, when the power is held at high power, are shown in Figures 5 and 6. Figure 5 shows the temperature field on the fuel and cladding for the reference meshed-crack model and the XFEM model. The results from these two models compare very closely, both for the overall solution as well as for the local thermal field in the vicinity of the crack in the cladding, which is the region of particular interest for a study on the effects of PCMI. In both cases, the temperature is very slightly suppressed on the inner surface of the cladding adjacent to the crack compared to the temperature at other locations on the inner surface of the cladding.

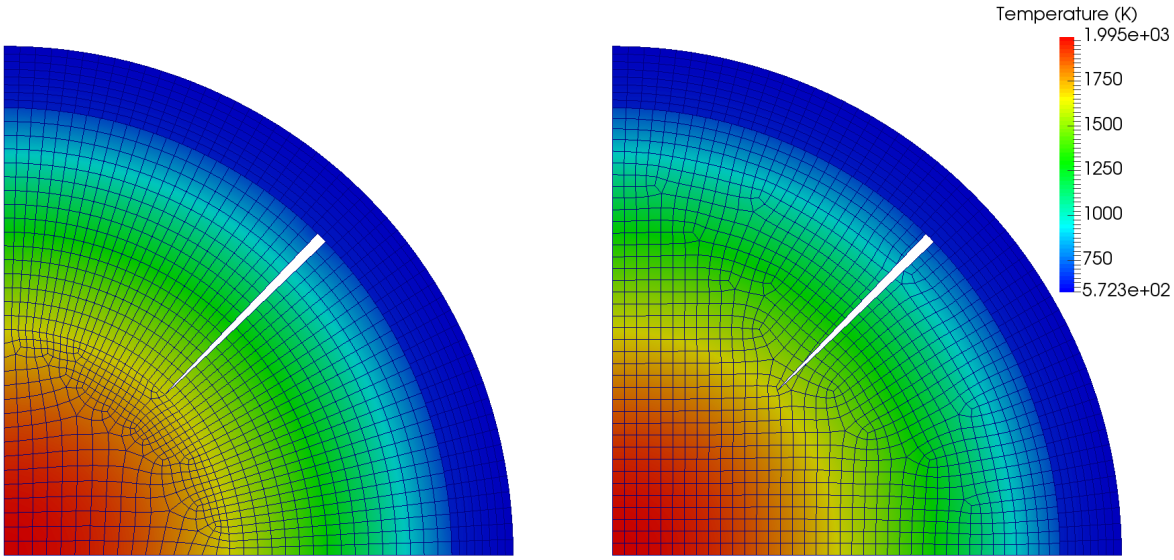

(a) Full model including fuel and cladding (meshed crack on left, XFEM crack on right)

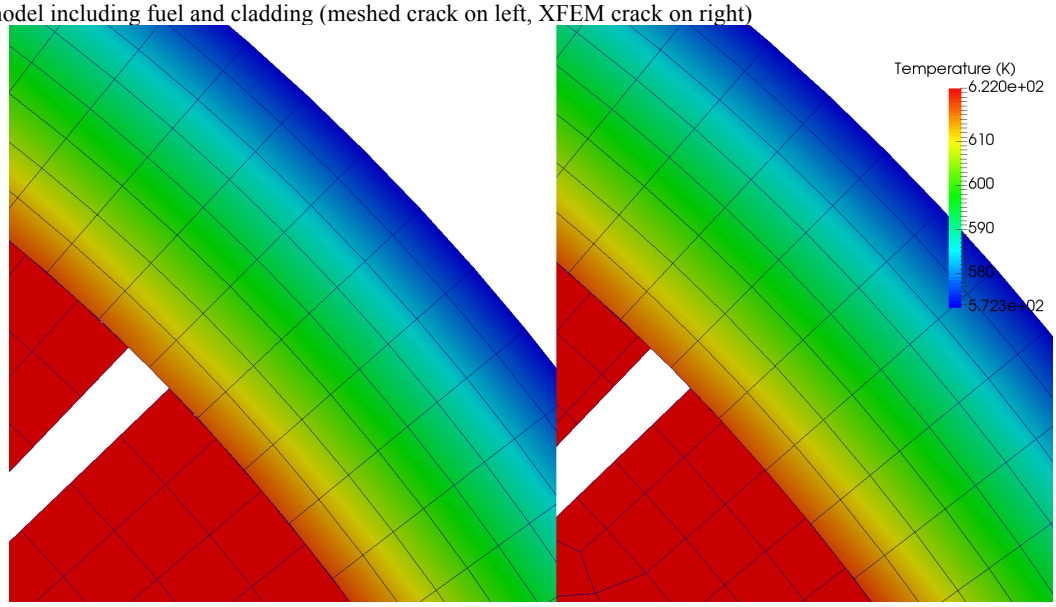

(b) Zoomed-in view fuel/cladding interface (meshed crack on left, XFEM crack on right)

FIGURE 5. Temperature fields in fuel and cladding at the end of the power history during a hold at high power.

Similar plots are shown for the von Mises stress field in Figure 6, with the results scaled for the full range of stresses in the fuel and cladding in Figure 6(a) and scaled just for the cladding in Figure 6(b). As for the thermal field, the solution results for the meshed crack and XFEM cases agree very well. The differences in the von Mises stress field obtained from these two models are plotted on the right in Figure 6(b), and the maximum errors are around 3%.

Because of the boundary conditions on these models, it is expected that the results should be symmetric about the crack plane. This is the case for the meshed crack case, but there are some slight departures from symmetry in the XFEM results. This is attributable to the fact that the meshing on the fuel outer surface is slightly biased to ensure that the crack would pass through an element rather than through a node. This departure from symmetry is quite minor, and both models capture the stress concentration induced by the presence of the crack in the fuel with very minor differences in the computed stress fields.

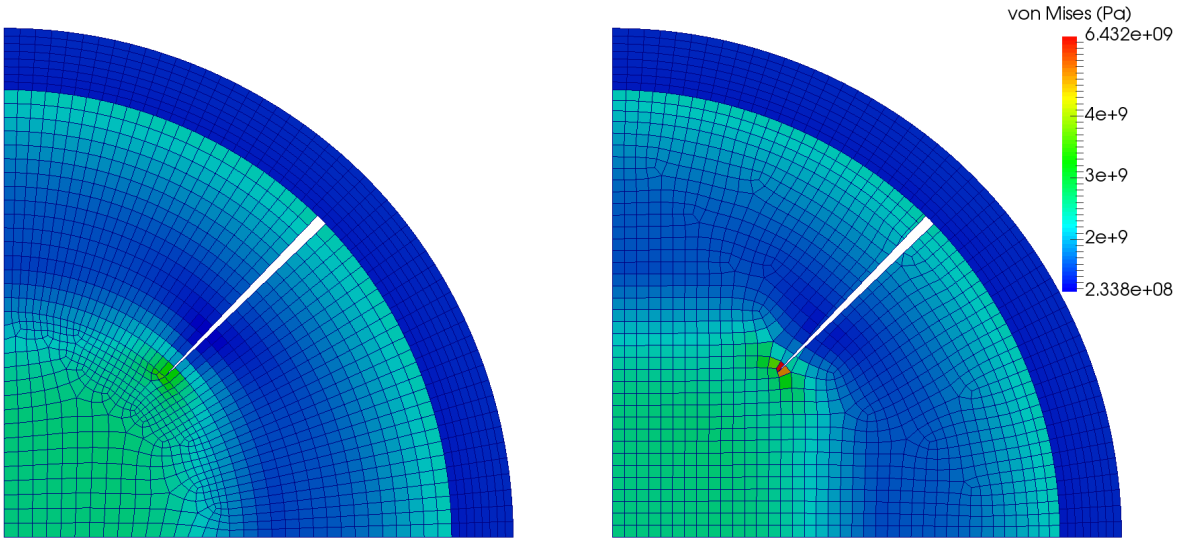

(a) Full model including fuel and cladding (meshed crack on left, XFEM crack on right)

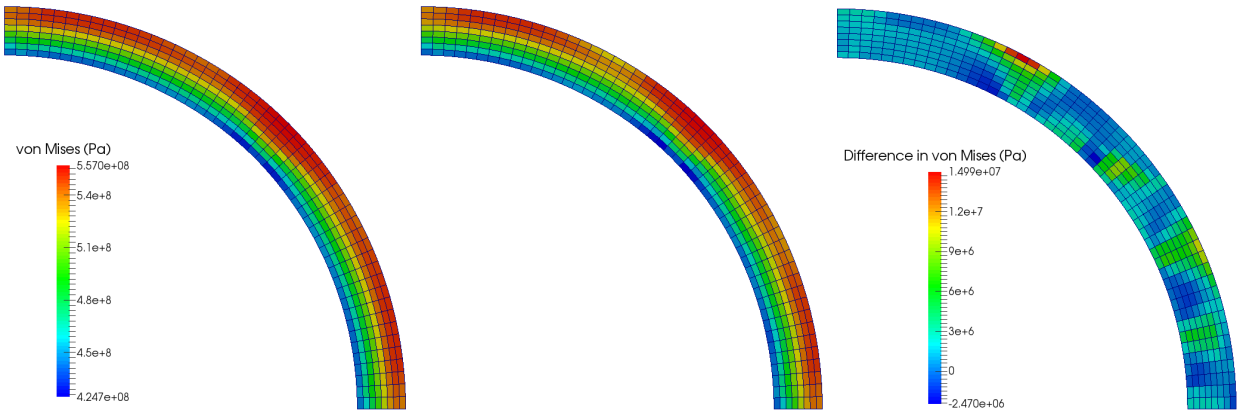

(b) Comparison of stresses in cladding showing von Mises stresses in meshed crack case (left) XFEM case (center), and difference between the two (XFEM subtracted from meshed crack). Maximum errors are roughly 3%.

FIGURE 6. von Mises stress fields in fuel and cladding at end of power history during a hold at high power.

CONCLUSION

This paper presents an initial demonstration of the use of the XFEM to represent the effects of a discrete crack in the fuel for an analysis of the cladding response in the vicinity of that crack due to PCMI. The XFEM has multiple benefits for this type of analysis, including its ability to represent propagating cracks and a simplified process for defining cracks without the need to create meshes that conform to the crack. The ability of the XFEM to accurately capture the effects of a crack on the response in the vicinity of the interacting surfaces of cracked fuel and cladding has been demonstrated both on simple benchmark problems and on a demonstration 2D cross-section model of a LWR fuel rod with a crack in the fuel. These models were all compared with benchmark solutions obtained from models with meshes conforming to a discrete crack. Good comparisons were obtained in all cases. There is still a need for further development of this capability, especially for including frictional contact effects, but this clearly demonstrates the utility and accuracy of XFEM for this type of analysis.

ACKNOWLEDGMENTS

This work was funded by the US Department of Energy under the Nuclear Energy Advanced Modeling and Simulation (NEAMS) and Consortium for the Advanced Simulation of Light Water Reactors (CASL) programs. The submitted manuscript has been authored by a contractor of the U.S. Government under Contract DE-AC07-05ID14517. Accordingly, the U.S. Government retains a non-exclusive, royalty free license to publish or reproduce the published form of this contribution, or allow others to do so, for U.S. Government purposes.

REFERENCES

[1] N. Capps, R. Montgomery, D. Sunderland, B. Spencer, M. Pytel, and B. Wirth. “Evaluation of missing pellets surface geometry on cladding stress distribution and magnitude.” Proc. WRFPM 2014, Paper No. 100109 (2014).

[2] N. Moes, J. Dolbow and T. Belytschko, “A finite element method for crack growth without remeshing,” *International Journal for Numerical Methods in Engineering,* **46**, 131-150 (1999).

[3] T. Belytschko and T. Black, “Elastic crack growth in finite elements with minimal remeshing,” *International Journal for Numerical Methods in Engineering*, **45**, 601–620 (1999).

[4] B. Spencer, H. Huang, J. Dolbow, and J. Hales. “Discrete modeling of early-life thermal fracture in ceramic nuclear fuel.” Proc. WRFPM 2014, Paper No. 100061 (2014).

[5] A. Hansbo and P. Hansbo, “A finite element method for the simulation of strong and weak discontinuities in solid mechanics,” *Compututer Methods in Applied Mechanics and Engineering*, **193**, 3523–3540 (2004).

[6] P. M. A. Areias and T. Belytschko, A comment on the article ‘‘A finite element method for simulation of strong and weak discontinuities in solid mechanics’’ by A. Hansbo and P. Hansbo (Comput. Methods Appl. Mech. Engrg. 193 (2004) 3523–3540). *Computer Methods in Applied Mechanics and Engineering* **195**,1275–1276 (2006).

[7] R. L. Williamson, J. D. Hales, S. R. Novascone, M. R. Tonks, D. R. Gaston, C. J. Permann, D. Andrs, and R. C. Martineau. “Multidimensional multiphysics simulation of nuclear fuel behavior,” *Journal of Nuclear Materials*, **423**, 149-163 (2012).

[8] http://www.mooseframework.org

[9] C. L. Richardson, J. Hegemann, E. Sifakis, J. Hellrung, and J. M. Teran, “An XFEM method for modeling geometrically elaborate crack propagation in brittle materials,” *International Journal for Numerical Methods in Engineering*, **88**,1042-1065 (2011).

[10] http://www.paraview.org

[11] B. Spencer, R. Williamson, D. Stafford, S. Novascone, J. Hales, and G. Pastore. “3D modeling of missing pellet surface defects in BWR fuel.” *Nuclear Engineering and Design*, In review.